Rheo-SAXS characterization of lead-treated oils: understanding the influence of lead driers on artistic oil paint's flow properties.

Lucie Laporte, Guylaine Ducouret, Frédéric Gobeaux, Arnaud Lesaine, Claire Hotton, Thomas Bizien, Laurent Michot, Laurence de Viguerie

Rheo-SAXS characterization of lead-treated oils: understanding the influence of lead driers on artistic oil paint's flow properties

Authors

Lucie Laporte [a*], Guylaine Ducouret [b], Frédéric Gobeaux [c], Arnaud Lesaine [a], Claire Hotton [d], Thomas Bizien [e], Laurent Michot [d], Laurence de Viguerie [a*]

[a]Laboratoire d'Archéologie Moléculaire et Structurale (LAMS), CNRS UMR 8220, Sorbonne Université, 75005, Paris, France
[b]Laboratoire Science et Ingénierie de la Matière Molle (SIMM), CNRS UMR 7615, ESPCI Paris, PSL Research University, 75005, Paris, France
[c]LIONS – NIMBE, UMR 3685 CEA/CNRS, CEA Saclay, 91191 Gif sur Yvette, France
[d]Laboratoire Physicochimie des Électrolytes et Nanosystèmes interfaciaux (PHENIX), UMR CNRS 8234, Sorbonne Université, 4 place Jussieu 75005, Paris, France
[e]Synchrotron SOLEIL, l'Orme des Merisiers, Saint-Aubin, 91192 Gif-sur-Yvette, France

*Corresponding author: lucie.laporte@sorbonne-universite.fr and laurence.de_viguerie@sorbonne-universite.fr

Abstract

From the 15th century onwards, painters began to treat their oils with lead compounds before grinding them with pigments. Such a treatment induces the partial hydrolysis of the oil triglycerides and the formation of lead soaps, which significantly modify the rheological properties of the oil paint. Organization at the supramolecular scale is thus expected to explain these macroscopic changes.

Synchrotron Rheo-SAXS (Small Angle X-Ray Scattering) measurements were carried out on lead-treated oils, with different lead contents. We can now propose a full picture of the relationship between structure and rheological properties of historical saponified oils.

At rest, lead soaps in oil are organized as lamellar phases with a characteristic period of 50 Å. Under shear, the loss of viscoelastic properties can be linked to the modification of this organization. Continuous shear resulted in a preferential and reversible orientation of the lamellar domains which increased with the concentration of lead soaps. The parallel orientation predominates over the entire shear range (0 – 1000 s^{-1}). Conversely, oscillatory shear coiled the lamellae into cylinders that oriented themselves vertically in the rheometer cell. This is the first report of such a vertical cylindrical structure obtained under shear from lamellae.

Keywords

Lead-treated oils, Supramolecular organization, Rheology, Rheo-SAXS (Small Angle X-ray Scattering)

Introduction

The oils used by painters, such as linseed oil, are said to be siccative, which means that they have the property to dry after a period of exposure to air. However, this drying is very slow, and can take up to several days. Painting with oil is therefore a long and tedious process [1], and until the 15th century, the technique was not very widespread and poorly mastered. It is at this point in time that painters began to treat their oils with driers before mixing them with pigments, in order to accelerate the

drying process [2]. Driers catalyse the polymerization of the film-forming compounds present in drying oils [3] which enabled oil painting to become a favoured medium. Studying the pre-treatments of oils, and the influence of these pre-treatments on the composition and properties of oils is of great importance to better understand complex paint systems. One common recipe involves adding a drier, and then heating the resulting mixture [4–7]. The driers are metal oxides, most often lead-based, such as lead (II) oxide PbO. Upon heating, a saponification reaction takes place: the presence of PbO triggers the saponification of the triglycerides in the oil and the formation of lead carboxylates (called lead soaps) [8,9]. The oil thus treated will polymerize ('dry') in a few hours [10]. Numerous physico-chemical properties of the oils, such as rheological properties, are modified by the formation of lead soaps [11]. Although the recipes have been known for centuries, changes in physical properties induced by metal soaps in oil have rarely been studied and quantified, and never linked to potential structural organization at the supramolecular scale.

Apart from the field of cultural heritage, studies carried out on the organization of triglycerides [12,13] can provide a solid methodological basis for the analysis of our systems. For example, structuring of fats for food application has been extensively studied. A thorough understanding of the structure/property relationship of fats allows developing products that meet precise specifications and has thus been a major research topic in the food processing industry [14]. It is assumed that triglycerides arrange themselves in pairs, with a double or triple fatty acid chain length structure. These pairs are stacked epitaxially to form lamellae, that finally self-assemble in lamellar domains [15–19]. The different structural assemblies of triglycerides and the influence of external parameters on crystallization was studied by Small Angle X-ray Scattering (SAXS) [20–22]. In addition, rheology has been used to study edible fats, which, as semicrystalline materials, exhibit a wide range of flow behaviors [23]. Rheo-SAXS, which corresponds to the coupling of the two previous techniques, allows correlating the supramolecular organization and the macroscopic properties of the studied systems and has then been used to understand the crystallization of fats [24].

Our goal in the present paper is to link the supramolecular organization of treated oils to their macroscopic behavior under shear. To do so, we formulated saponified oils and characterized their rheological behaviors. The influence of the initial lead oxide proportion was investigated, and particular attention was given to sample with viscoelastic properties. To explore the structure/rheological properties relationship of lead-treated oils, SAXS was performed on sample at rest and under shear using the Rheo-SAXS equipment available on the SWING beamline at Synchrotron SOLEIL. The impact of continuous and oscillatory shear on supramolecular organization was investigated. The supramolecular structure of treated oils under shear could be elucidated and correlated to the different stages of paint application (at rest and under the brush).

Materials and methods

Sample formulation

The linseed oil was an untreated cold pressed oil from Kremer (ref. 73020). The composition of fatty acids is given by the provider as: linolenic acid 61.3 %, oleic acid 15.3%, linoleic acid 14.6 %, palmitic acid 4.4%, stearic acid 2.9% and others (being < 0.5 %) 1.5%.

The samples were formulated in batches of 20 g. Lead (II) oxide PbO (Emsure) was first pre-ground with 2 mL of untreated cold pressed linseed oil in a porcelain mortar for 20 seconds. The remaining oil was then added and the mixture was ground for 40 additional seconds. The mixture was transferred to a 100 mL beaker and heated in a silicone oil bath at a control temperature of 150°C, under magnetic stirring. For samples containing more than 17 mol% PbO, the lead (II) oxide was dispersed manually during the first 30 minutes of heating to avoid the formation of a sticky

unreacted PbO deposit. At the end of heating, the treated oil was immediately poured into a glass pillbox and left to cool at ambient temperature. To investigate the influence of the initial PbO concentration, formulations containing 1, 5, 10 and 20 wt%, (corresponding to 4, 17, 31 and 50 mol%, respectively) were prepared. Such a concentration range is representative of the recipes for treated oils from the 15th to the 19th century. Above 10 wt% PbO, the treated oil was not used directly as a binder for paints, but as a medium: it was directly added to a paint in order to adjust its consistency. In the following, the concentrations will be expressed in molar percent of initial PbO. The saponification rate (i.e. the percentage of saponified ester bonds) was determined by FTIR (Fourier-Transform InfraRed spectroscopy) for all the formulated samples (3 measurements per sample), following a method described in detail elsewhere [9]. To avoid any effect related to the aging of samples, the measurements presented in this paper were performed on "fresh" samples, at the latest ten days after formulation. Between measurements, the samples were stored at 4°C in sealed pillboxes under inert gas (N_2).

Rheology

Rheology measurements were carried out on a Thermo Fisher Scientific HAAKE MARS 40 controlled stress rheometer, equipped with a sand blasted stainless steel cone-plate geometry (diameter: 35 mm, angle: 2°; gap: 0.104 mm). Measurements were performed at 25°C, the temperature being maintained by an air Peltier module. Each measurement was repeated at least twice to check reproducibility. Another sample with the same composition, prepared in the same conditions, was also analysed and its properties compared to the first one. Indeed, two samples with the same composition present similar behaviour, but a maximum deviation of 30% can be observed for *G'* and *G''* values. To verify that measurements in cone-plate and Couette geometry yield similar results, some measurements were also carried out with a rheometer equipped with a Couette cell, in configuration identical to that of the Rheo-SAXS device described below. Two samples of each formulation were prepared in the same condition and the results were compared to check the reproducibility. Data acquisition and processing were performed using RheoWin 4.87.

Flow measurements were performed according to the procedure described by de Viguerie *et al*. [25] and Plisson *et al.* [26]. Shear rate sweep tests were then performed from 0.01 to 1000 s^{-1}. If needed, flow measurements were carried out with both increasing (ramp up) and decreasing (ramp down) shear rate. For long-lasting measurements, a hermetic cell was placed around the geometry to limit contact between the sample and ambient air and thus prevent drying.

Dynamic measurements were performed on viscoelastic samples, as follows:

1. A first strain sweep test from 0.05 to 1000% strain was carried out at f = 1 Hz to evaluate the extent of the linear regime.
2. A new sample was then used to carry out a second strain sweep test from 0.05% strain and stopped before the end of the linear viscoelastic plateau, at f = 1 Hz, to ensure the reproducibility of the first strain sweep test.
3. Finally, frequency sweep test from 0.1 to 100 rad/s at constant strain of 1% was performed.

Additional tests were performed on the viscoelastic samples to evaluate their restructuring: samples were submitted to a strain sweep test from 0.1 to 1000% strain at f = 1Hz. Measurements of G' and G'' from 0.1 to 0.5% strain were then carried out over time to assess possible sample restructuring.

Rheo-SAXS

Rheo-SAXS measurements were performed on the SWING beamline of the SOLEIL synchrotron (Gif-sur-Yvette, France). Shearing of the samples were coordinated with the acquisition of the corresponding SAXS signal. An illustration of the measurement principle is shown below (Figure 3.a).

The rheometer set on the beamline was a controlled stress rheometer MCR 501 (Anton Paar). Samples were loaded into a Couette cell with a 500 µm gap, consisting of a rotating inner cylinder and a static outer cylinder. The total immersed height was 18 mm. The rotor and stator are made of polycarbonate, to ensure a correct transmission of both incident and scattered X-rays.

- For flow measurements, each used shear rate value (1, 10, 100, 1000 s^{-1}) was applied for 10 minutes, and rheological data were monitored to ensure that the sample does not undergo any significant change over time.
- For dynamic measurements, the oscillatory shear was applied under the same conditions as for the HAAKE MARS 40, and SAXS acquisitions were done on the fly.

SAXS measurements were performed at a constant beam energy of 12 keV. For each applied shear rate or strain value, two-dimensional SAXS patterns (5 frames acquisition per image, 1000 ms of exposure time) were recorded both in the radial and tangential configurations using an EigerX4M detector (Dectris) with a 75x75 mm^2 pixel size. The sample to detector distance was fixed at 0.9 m. In such condition, the accessible q range, q being the scattering vector ($q = 4\pi \, sin\theta/\lambda$, where 2θ is the scattering angle and λ the wavelength) extends from 0.007 to 0.7 $Å^{-1}$ after mask application. In the radial configuration, the beam crosses 1 mm of sample (twice the gap) whereas the total sample thickness in the tangential configuration is around 2 mm. The obtained images were treated using two different integration procedures (Figure 3.a):

1. Azimuthal integration: in this procedure, an angular integration is performed. For isotropic samples, the integration covered 360° whereas for anisotropic samples, the integration was performed in a cake, the opening of which was adjusted depending on the sample. Such a procedure yields curves in which the scattered intensity is plotted versus the scattering vector modulus *q.*
2. Azimuthal profile: to quantify anisotropy, the scattered intensity at a given scattering vector modulus q is plotted as a function of ψ ($\psi \in$ [0, 360°] in steps of 2°). The q value chosen was that where anisotropy is maximal in the systems, *i.e.* 0.15 ± 0.01 $Å^{-1}$.

All profiles obtained were normalized in transmission and thickness and the contribution of the empty Couette cell was subtracted. 2D images were processed using Foxtrot 3.5. The 1D obtained spectra were analysed using SASView 5.0.4 and Fityk 1.3.1.

Results and discussions

Heating the oil at 150°C in presence of PbO leads to the partial saponification of the triglycerides and free fatty acids present in the oil. We present here the results for different formulations prepared from 0 to 50 %mol of PbO, which correspond to different saponification rates calculated from the FTIR spectra [9] indicated in Table 1. Other reactions also occur such as oxidation, isomerization, cleavage and oligomerisation that induce the formation of a wide variety of different molecules [27] included in what is called below as the “oil matrix”.

Table 1 : Final saponification rate of linseed oil samples heated at 150°C with PbO as a function of the initial amount of PbO.

PbO init. (% mol.)	4	17	31	50
τ_s (%)	3 ± 0	18 ± 2	33 ± 3	59 ± 4

Rheology

Uncooked linseed oil, taken as a reference, behaved like a Newtonian fluid, with a viscosity of about 40 mPa.s (Figure 1.a). Oil cooked at 150°C was slightly more viscous, its viscosity was close to 55 mPa.s. Lead soaps were responsible for a pronounced increase in viscosity: at a given shear rate, the

viscosity of treated oils increased with PbO concentration. Systems containing 4 to 31 mol% PbO still exhibited a Newtonian behavior, with viscosity between 135 and 155 mPa.s, and their flow properties did not vary with time and sample shearing history. In contrast, the linseed oil cooked with 50 mol% PbO displayed an increase in viscosity at low shear rate and a shear thinning behavior. As suggested by de Viguerie *et al.* [25], this behavior indicates lead soaps' structuring at the supramolecular scale. At low shear rates, it induces an increase in viscosity, while at high shear rates, the viscosity tends to a plateau, suggesting an evolution of the organization under applied stress.

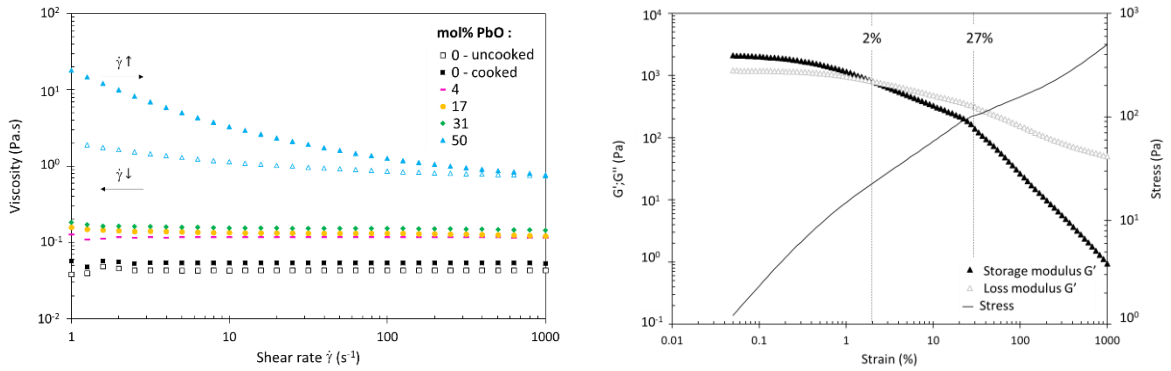

(a) (b)

Figure 1 : (a) Flow tests on linseed oils cooked with various amounts of PbO, expressed in molar percentage, from 0 to 50 mol%. For the sample linseed oil + 50 mol%, solid symbols and hollow symbols correspond to ramp up and ramp down measurements respectively. Error bars are smaller than the symbols size and thus not visible (b) Strain sweep test from 0.05 to 1000 % (f = 1 Hz) in Couette geometry on linseed oil + 50 mol% PbO.

The flow properties of the most saponified sample, linseed oil + 50 mol% PbO, varied depending on its shear history. Flow measurements with decreasing shear rates (ramp down) were therefore performed. No reversibility was observed between the ramp up and the ramp down: once sheared, the sample did not recover its initial properties. The same trend is observed for slow flow measurements (total time measurement of about 20 hours, see Supporting Information Figure 2). The initial supramolecular organization was thus partially modified under the continuous shear.

Moreover, unlike the less saponified samples, the linseed oil + 50 mol% PbO exhibited a plastic behavior: it did not flow at rest, and its yield stress ranked between 5 and 10 Pa, which is comparable to most commercial paints [28].

From 0.05 to 0.5% strain, G' was higher than G'' and the value of both moduli was approximately constant (Figure 1.b): this is the linear viscoelastic plateau (LVP). At 0.5%, as the LVP domain ended, the values of G' and G'' decreased until G' was lower than G'' (crossing at 2% strain): the system became viscous and flowed, sign of a first destructuring at the supramolecular scale. Another change of slope was observed at 27% strain, indicating a second destructuring. To determine if the sample could recover its viscoelasticity, we measured the evolution of G' and G'' over time at low strain (0.5%) on the previously sheared sample (see Supporting Information Figure 3): the elastic and viscous moduli reached threshold values of 250 and 200 Pa respectively after 5h, corresponding to 15% and 19% of their initial value. No significant change was observed afterwards.

Structuring of lead soaps

At rest

As expected, linseed oil alone did not display any organization (Figure 2.a) : the broad and diffuse peak centred around q = 0.27 $Å^{-1}$ (i.e. d = $2\pi/q$ = 23 Å) corresponds to the average correlation

distance between polar parts of triglycerides [29]. In contrast, the SAXS data of partially saponified oil at rest, and particularly on the linseed oil + 17 mol% PbO sample, exhibited peaks at q = 0.13, 0.26 and 0.39 $Å^{-1}$. Such values, that are periodic with a q ratio of 1:2:3, are typical of a lamellar organization [30], whose characteristic distance d given by $d = 2\pi/q$, with q the position of the first peak. Here, the period of the lamellar phases was then of the order of 50 Å, which corresponds to the size of an extended C18 lead soap [31,32]. On the samples containing linseed oil + 31 mol% PbO and linseed oil + 50 mol% PbO, the harmonics were partly masked by a broad peak centred at 0.20 $Å^{-1}$ (i.e. 31 Å), probably linked to unorganized lead soaps. The influence of the initial PbO concentration on the position of the different signals (lamellar and unorganized lead soaps) will not be discussed here and will be covered in another paper. At rest, lead soaps are thus organized in lamellar phases, and their organization is likely to evolve under shear [33].

Continuous shear

These same samples were submitted to continuous shear of 1, 10, 100 and 1000 s^{-1}, with increasing and decreasing shear rate. The evolution of azimuthal integrations and azimuthal profiles allowed probing the evolution of lamellar organization under shear.

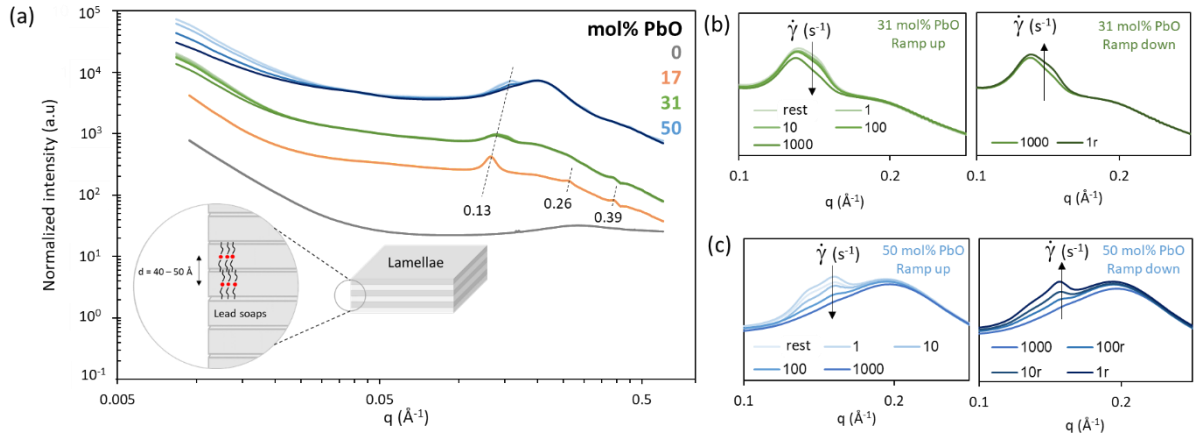

Figure 2 : (a) Scattering curves of partially saponified oils with different initial amount of PbO. The insert shows the organization of the lead soaps into lamellar phases at rest. Blow-up on the evolution of the fundamental peak of the lamellar organization under continuous shear, for (b) 31 mol% PbO and (c) 50 mol% PbO. The "r" refers to shear rate values applied on ramp down.

Whatever the shear applied, the least saponified sample linseed oil + 17 mol% PbO displayed an unchanged scattering curve, and the 2D-scattering pattern remained isotropic (see Supporting Information Figure 4). The shear did not affect the supramolecular organization of the sample, and lamellar domains remain randomly oriented in the Couette cell.

In contrast, samples with higher concentrations of lead soaps showed an attenuation of the first-order lamellar peak as shear increased. The more saponified the sample was, the stronger this effect was. For linseed oil + 31 mol% PbO, a slight attenuation was detected at 1000 s^{-1} (Figure 2.b).

As for linseed oil + 50 mol% PbO (Figure 2.c), the attenuation was visible from 1 s^{-1}. At 1000 s^{-1}, the lamellar signal had completely vanished. This evolution of the scattering curves was associated to a change in the azimuthal profiles: at rest, all 2D SAXS images were isotropic, i.e. the lamellar domains were randomly oriented. Linseed oil + 17 mol% PbO sample did not exhibit anisotropy at any shear rate (see Supporting Information Figure 4). Conversely, anisotropic scattering patterns were observed for the linseed oil + 31 and 50 mol% PbO samples under shear (Figure 4), meaning that the lamellar domains adopted a preferential orientation. The lamellae can be oriented in three distinct ways, called parallel, perpendicular and transverse [34]. Each orientation is characterized by a

specific combination of patterns obtained in radial and tangential configurations (Figure 3.b). Usually, parallel and perpendicular orientations are dominant for lamellae under shear [35,36].

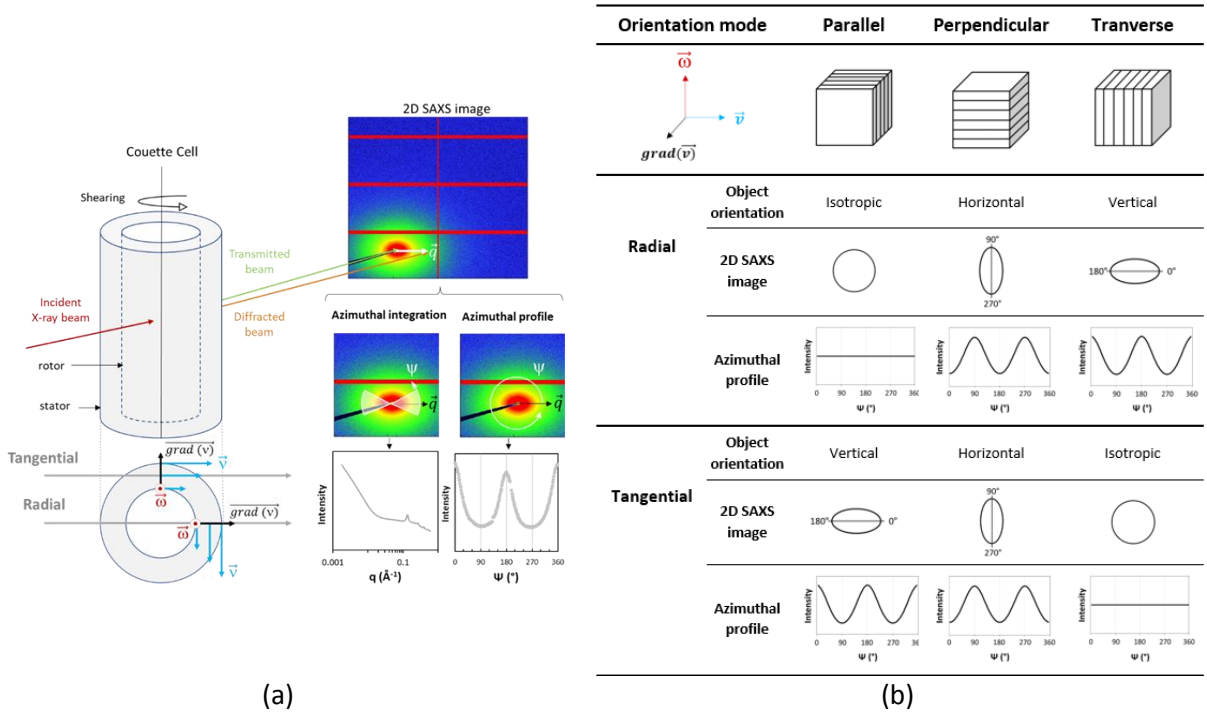

(a) (b)

Figure 3 : (a) Rheo-SAXS measurement principle and schematic representation of 2D SAXS image treatment (b) Schematic representation of the 2D SAXS image in radial and tangential configuration corresponding to the three possible orientations of the lamellar domains

For the linseed oil + 31 mol% PbO sample, the signal in radial configuration remained isotropic, while in tangential configuration, the profile was characteristic of a vertical orientation of the lamellae (Figure 4.a). This trend was more pronounced at 1000 s^{-1}. The combined radial and tangential data were characterized a parallel orientation of the lamellae.

For the linseed oil + 50 mol% PbO sample (Figure 4.c), the same trend was observed in the tangential configuration: a vertical orientation of the objects was visible. The anisotropy increased with shear rate, along with the attenuation of the first order lamellar peak. However, contrary to the less saponified samples, the azimuthal profile in radial configuration was not isotropic. At rest, the observed anisotropy is characteristic of vertically oriented lamellae in the cell. From 1 to 10 s^{-1}, this anisotropy increased. At 100 s^{-1}, a transition occurred and the anisotropy evidenced the presence of horizontally oriented objects in the cell, a feature that was more pronounced at 1000 s^{-1}. This weak anisotropy observed in radial configuration can be assigned to the coexistence of two orientation modes of the lamellar domains.

From 0 to 10 s^{-1}, the vertical orientation detected in radial configuration indicates that a minor part of the lamellar domains was oriented transversely to the Couette cell. A change of orientation happened from 10 to 100 s^{-1}: horizontal orientation detected in radial configuration shows that a fraction of the lamellar domains was aligned perpendicular to the Couette cell, and the horizontal orientation expected in the tangential configuration was masked by the more abundant vertically oriented lamellae in the parallel orientation.

Such a coexistence of parallel and perpendicular orientation had already been observed by Poulin *et al.* on more rigid systems, such as graphene oxides [37]. The transverse orientation is generally not observed during shearing of lamellar phases because it is unstable : the applied shear forces lamellae

to deviate from their characteristic equilibrium distance, which induces their deformation and rupture [38,39]. Here, we assume that the filling of the Couette cell had an influence on the orientation of the lamellae detected at low shear rates: during the vertical descent of the rotor prior to the measurement, a fraction of the lamellae oriented themselves transversely, then reoriented themselves perpendicularly at high shear rates.

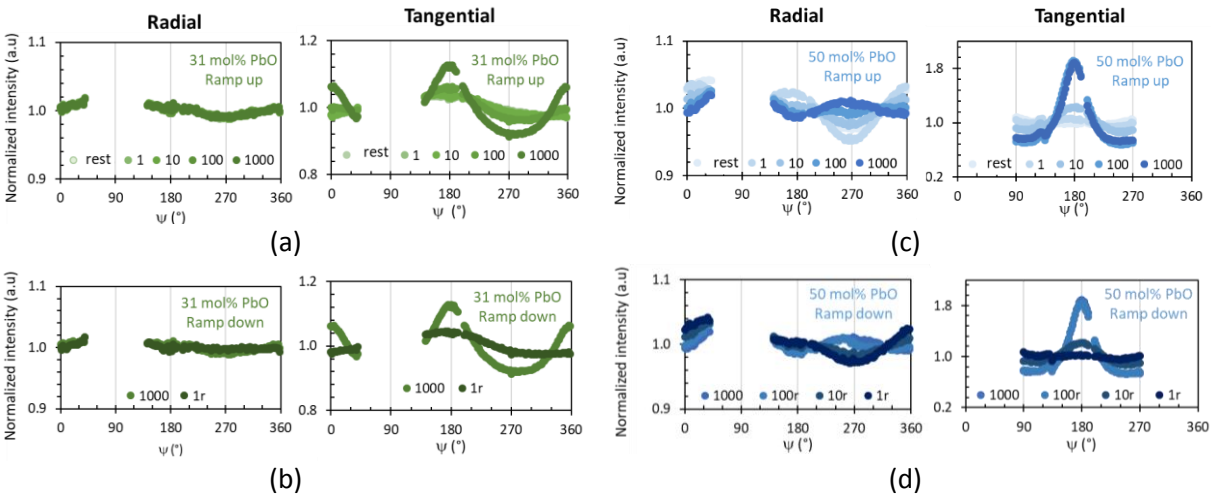

Figure 4 : Evolution of azimuthal profiles under continuous shear for linseed oil + 31 mol% PbO ramp up (a) and ramp down (b), and for linseed oil + 50 mol% PbO ramp up (c) and ramp down (d). The first line corresponds to the ramp up (1 to 1000 s^{-1}) and the second line to the ramp down (1000 to 1 s^{-1}). The missing points are due to the junctions between the detectors and to the beamstop. The "r" refers to shear rate values applied on ramp down.

When subjected to continuous shear, the lamellar domains thus adopted preferential orientations, resulting in an evolution of both the azimuthal profiles and the intensity of the first order lamellar peak. The orientation mode depended on both the saponification rate of the sample and the applied shear rate. For the linseed oil + 17 mol% PbO sample, no preferential orientation was observed. Two hypotheses can explain this trend: the sample being less saponified, it contained isolated lamellar domains without connection between them. They therefore have more degrees of freedom to orient themselves freely in the cell, even under shear. In addition, the linseed oil + 17 mol% PbO had a low viscosity: when sheared, the lamellae were free to move and aligned themselves in the shear plane. On the contrary, the linseed oil + 50 mol% PbO sample was highly concentrated in lamellar phases interacting together: under shear, they were organized in "layers" parallel to the shear plane, that could slide on each other at high shear rates, which gave the sample its shear-thinning behavior.

The modifications observed on the SAXS profiles of samples linseed oil + 31 % PbO and linseed oil + 50 mol% PbO were reversible. On the ramp-down, the intensity of the lamellar peak increased until it reached 100 % of the initial area (Figure 2.b and 2.c). Similarly, the azimuthal profiles of the ramp down were close to those of the ramp up at a given shear rate (Figure 4.b and 4.d). When shear is stopped, there is no more preferential orientation of the lamellar domains. Surprisingly, as seen in Figure 1.a, viscosity is not reversible between the ramp-up and ramp-down for the linseed oil + 50 mol% PbO, even though the shear steps applied were long (see Supporting Information Figure 2). We can then assume that the irreversible destructuring occurred at a different scale than the one probed in SAXS. Dense packing of lamellar domains may have been irreversibly broken under shear, without the internal structuring of lamellar domains being destroyed.

Oscillatory shear

We then focused on the linseed oil + 50 mol% PbO sample because of its viscoelastic properties. The sample was submitted to a strain sweep test with strain increasing from 0.05 to 1000% (frequency =

1 Hz). Slope changes observed at 2 and 27% strain (Figure 1.b) suggest a modification of the organization of the lead soaps during oscillatory shear.

The viscoelastic properties of linseed oil + 50 mol% PbO were then linked to SAXS measurements. From 0.05 to 20% strain, the signal increased sharply from ca. 0.007 to 0.1 $Å^{-1}$ (Figure 5.a), which showed that lead soaps structured into objects of increasing dimensions, that may be approximated by the Guinier relation [40,41]. Guinier fits were performed on SAXS profiles from $q \in$ [0,01 - 0,10 $Å^{-1}$], according to the model:

$$I(q) = A \cdot \exp\left[-\frac{q^2 Rg^2}{3}\right] + B \ \#(1)$$

with Rg the radius of gyration ($Å^{-1}$), A the scale factor or volume fraction (adimentioned), and B the source background (a.u). The formed objects reached a radius of gyration of 39 Å at 20 % strain (Figure 5.b). Beyond 20% strain, the growth of the objects was slight (39 to 44 Å, see Supporting Information Figure 5).

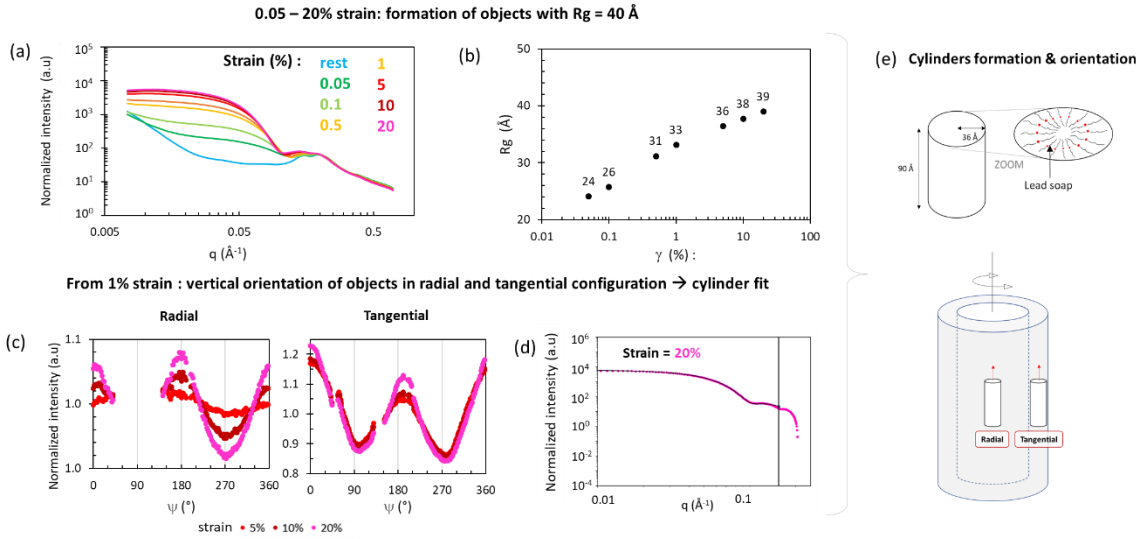

Figure 5 : Rheo-SAXS on linseed oil + 50 mol% PbO - SAXS profiles, (a) measurements in radial position (data in tangential configuration are similar) from 0 to 20% strain at f = 1Hz. (b) Corresponding radius of gyration Rg according to the Guinier model. (c) Azimuthal profiles, from 5 to 20% strain. (d) Cylindrical fit on the SAXS profile at 20% strain. The signal of the sample at rest is subtracted. (e) Schematic representation of the cylindrical objects formed. Dimensions correspond to the results of the 20% strain fits.

For the past three decades, the structuring of surfactants under shear has been an important research topic. Indeed, surfactants may form supramolecular structures suitable for the encapsulation of active substances for drugs or detergents for instance [42]. In 1993, Diat and Roux [43] thus showed that multilamellar vesicles (MLVs) could be formed by shearing a lamellar phase of anionic surfactants. Similar transitions were observed with other surfactants (non-ionic and cationic) [33,35,44,45]. In our case, the formation of MLVs is not compatible with the observed evolution of anisotropy. Indeed, from 1% strain, both tangential and radial azimuthal profiles are characteristic of vertically oriented objects in the Couette cell (Figure 5.c). We therefore postulated the formation of vertically oriented cylindrical objects in the cell. To verify this hypothesis, fits were performed on the signal of the sheared sample, from which the signal of the sample at rest was subtracted, in order to consider only the organizations formed during shearing. We fitted the data with SASView by applying the cylinder model [46,47].

The fits were indeed consistent with vertically aligned cylinders in the cell (Figure 5.d and 5.e). It can be assumed that these cylinders resulted from the curvature of the lamellae under oscillatory shear. These cylinders formed at very low strain amplitudes and then oriented themselves in the Couette cell from 1 to 5% strain. This transition between the two morphologies occurs at the intersection between G' and G'' detected in strain sweep test (Figure 1.b).

Considering this model, we can explain the evolution of the anisotropy over the whole strain range: from 0.05 to 1% strain, the tangential signal is characteristic of a vertical orientation (Figure 6.a). In the radial configuration, the profile is characteristic of a horizontal orientation. We can therefore assume that a majority of the lamellae were oriented parallel to the walls of the cell, and were responsible for the tangential anisotropy. However, if all the lamellae were indeed oriented parallel to the cell walls, no anisotropy would be observed in the radial configuration. A fraction of the lamellae was thus oriented perpendicularly to the cell wall, responsible for the anisotropy in the radial configuration. This anisotropy was weaker than the one observed tangentially, so the perpendicular orientation mode concerned only a small proportion of the lamellae, and the parallel orientation predominated in the deformation range studied. It is interesting to note that the radius of the cylinders at 20% strain corresponds approximately to the length of a lead soap (Figure 5.e). However, considering previous Rheo-SAXS studies on lamellar systems, one would expect the formed objects to be multilamellar. Indeed, formation of MultiLamellar Cylinders (MLCs) has been evidenced under constant shear of lamellar phases of non-ionic surfactants [33,45]. In our case, the following scheme can be proposed: oscillatory shear would cause delamination of the lamellar domains prior to cylinder formation. At low strain, lamellar domains oriented themselves parallel to the cell wall, and then lamellae would slide over each other. Each lamella would coil to form a unilamellar cylinder oriented vertically in the cell. It can thus be assumed that the parallel orientation of the lamellae favoured the formation of cylinders. From 1% strain, the amount of cylinders formed was sufficient for the vertical anisotropy of the cylinders to predominate over the parallel alignment of the remaining lamellar phase. This structural change correlates with the loss of viscoelastic properties observed at 2% strain (Figure 1.b). The cylinders continued to form until 20% strain.

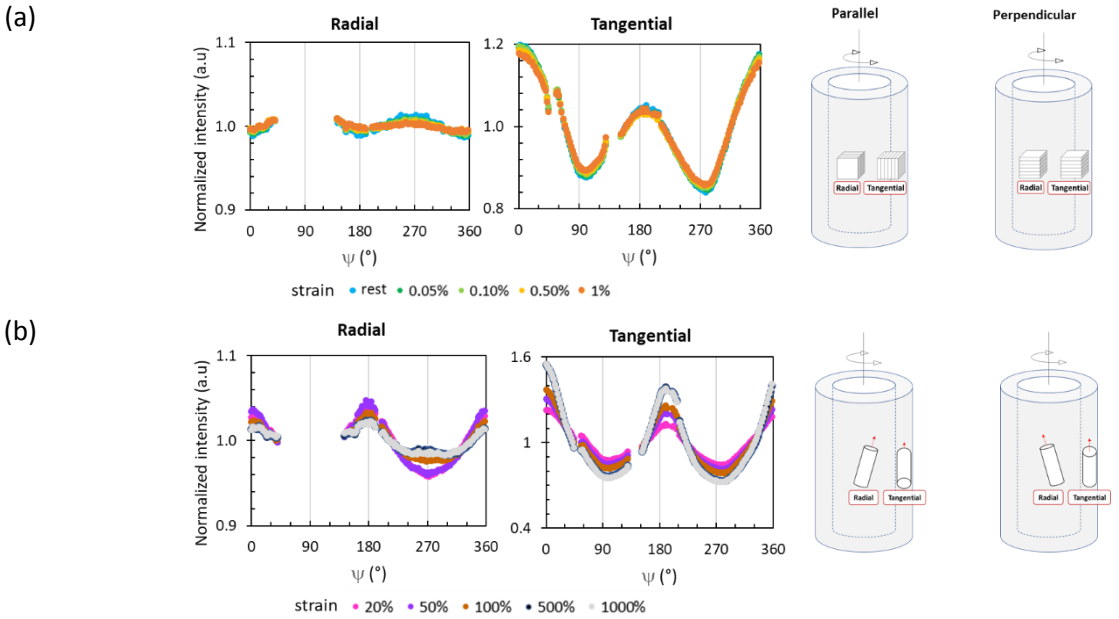

Figure 6 : (a) Azimuthal profiles on linseed oil + 50 mol% PbO, from 0,05 to 1% strain (f = 1Hz), showing a coexistence of orientation of lamellar phases. (b) Azimuthal profiles on linseed oil + 50 mol% PbO, from 20 to 1000% strain (f = 1Hz), showing a disturbed vertical orientation at high strain. All azimuthal profiles were plotted for q = 0.15 ± 0.01 Å $^{-1}$

Beyond 20% strain, the growth of the cylinders was slight, but the anisotropy evolved significantly (Figure 6.b): it decreased in the radial configuration and increased in the tangential configuration. We thus suppose that the vertical alignment previously observed in the radial configuration was disturbed at too high strain, because the cylinders oscillated in the shear plane direction. This second transition is associated with the second slope break of *G'* and *G''* measured in rheology at 27% strain (Figure 1.b).

The structuring of lamellar phases of lead soaps under oscillatory shear significantly differed from what has been reported for other lamellar systems. Most studies on lead soaps have focused on the behavior of straight saturated chains, without considering the potential effect of unsaturation on supramolecular organization [48,49]. Moreover, here, we do not consider pure lamellar systems but rather a complex mixture whose constituents have opposite behaviors. On one hand, lead soaps are able to organize themselves at the supramolecular scale. On the other hand, these lead soaps are surrounded by partially hydrolysed and unorganized triglycerides that can hinder this structuring. Considering the unorganized surrounding oil is thus essential for a proper representation of real systems. The formation of MLVs has been extensively studied by application of constant or increasing continuous shear on lamellar phases of surfactants. One pattern prevails [35,44]: beyond a certain stress, the initial lamellar phase cannot handle the deformation and therefore evolves into a new state, called "onion phases", where all the space is filled by MLVs. The appearance of MLVs is marked by an increase in viscosity. The MLVs can then pack hexagonally and eventually re-fracture into lamellar phases. Under oscillatory shear, the pattern is similar but the formation of MLVs is conditioned by the application of a minimum deformation amplitude and is characterized by a strong viscoelasticity [42].

Ito *et al.* [45] demonstrated the formation of MLCs as an intermediate structure between the perpendicular orientation of lamellae under shear and the formation of MLVs. However, in the case they report, the orientation of the detected cylinders was horizontal, which significantly differs from our observations. It has also been proposed that the characteristic SAXS profile of cylindrical objects could actually correspond to a coherent undulation of the lamellae (called "stripe buckling"). Both

situations lead to similar SAXS signals. In order to check if this applies to our systems, we extended the SAXS data acquisition for 30 minutes after the end of the oscillatory shear. The SAXS data did not evolve significantly with time as the vertical orientation remained in both radial and tangential configurations (see Supporting Information Figure 6). Objects with radius of gyration of ca. 44 Å are still present (see Supporting Information Figure 7). It then appears that the cylindrical objects are not related to coherent undulations of lamellae.

Conclusion

This work enabled us to depict the structure/property relationship of a historical paint medium, and gain new insights on systems, previously only described from a molecular or macroscopic perspective [9–11,25,26]: we have shown how saponified oil behaves at rest and under stresses corresponding to those applied by the painter's brush. It appears that the lamellar organization identified at rest evolves in a different way depending on the type of shear applied. Continuous shear leads to an alignment of the lamellar phases, whereas under oscillatory shear, the lamellae progressively structure themselves into vertically oriented cylindrical objects in the rheometer cell. This is the first report of vertically oriented cylinders formed from lamellae under shear: this result obtained from a complex functional lamellar system, lamellar domains dispersed in an unorganized oil matrix, contrasts with the more commonly observed multi-lamellar vesicles formed after shearing of ideal pure lamellar phases [35,43,44]. According to earlier work on these multi-lamellar vesicles [33,45], they are formed as a result of the evolution of intermediate horizontal multi lamellar cylinders, and are preserved after shear. In our case, further investigation is planned to monitor the stability of these cylindrical structures at rest after shear and to link them to the observed partial recovery of viscoelasticity. Chromatographic analyses are also in progress in order to finely characterize the chemical composition of the different saponified oils studied and to further discuss the influence of the composition on the supramolecular organization of the systems. The influence of inorganic particles of pigments on this organization should also be explored in order to gain a better insight into painters' practices.

Acknowlegements

This project was funded by Sorbonne Université. The Rheo-SAXS experiment was performed with the approval of the SOLEIL Peer Review Committees (Proposal No. 20201202). The SWING beamline staff is thanked for allowing us to collect data at their workstation, and for their support and assistance during and after the beamtime.

References

[1] Theophilius Presbyter, J.M. Giuchard, C. de L'Escalopier, Diversarum artium schedula, Brockhaus et Avenarius, Leipzig, 1843.

[2] G. Vasari, C. Weiss, Les vies des plus excellents peintres, sculpteurs, et architectes, Dorbon-Aine, Paris, 1900.

[3] J.H. Bielman, Driers, in: Surf. Coat. Vol. 1 Raw Mater. Their Usage, Springer Netherlands, Dordrecht, 1993: pp. 592–610. https://doi.org/10.1007/978-94-011-1220-8_33.

[4] M. Faidutti, C. Versini, Le Manuscript de Turquet de Mayerne présenté par M. Faidutti et C. Versini, Pictoria Sculptoria et quae subalternarum artium -1620, Audin Imprimeurs, Lyon, 1967.

[5] M.P. Merrifield, Original Treatises: Dating from the XIIth to XVIIIth Centuries on the Arts of Painting, in Oil, Miniature, Mosaic, and on Glass; of Gilding, Dyeing, and the Preparation of Colours and Artificial Gems, John Murray, Albemarle Street, 1849.

[6] C.L. Eastlake, Materials for a history of oil painting, Longman, Brown, Green, and Longmans, London, 1847.

[7] L. Carlyle, The artist's assistant : oil painting instruction manuals and handbooks in Britain 1800-1900, with reference to selected Eighteenth-century sources, Archetype Publication, London, 2001.

[8] M.R. Mills, An Introduction to Drying Oil Technology, Pergamon press LTD, London, 1952.

[9] M. Cotte, E. Checroun, J. Susini, P. Dumas, P. Tchoreloff, M. Besnard, Ph. Walter, Kinetics of oil saponification by lead salts in ancient preparations of pharmaceutical lead plasters and painting lead mediums, Talanta. 70 (2006) 1136–1142. https://doi.org/10.1016/j.talanta.2006.03.007.

[10] L. de Viguerie, P.A. Payard, E. Portero, P. Walter, M. Cotte, The drying of linseed oil investigated by Fourier transform infrared spectroscopy: Historical recipes and influence of lead compounds, Prog. Org. Coat. 93 (2016) 46–60. https://doi.org/10.1016/j.porgcoat.2015.12.010.

[11] I. Kneepkens, Understanding historical recipes for the modification of linseed oil, University of Amsterdam, 2012.

[12] M.M. Alam, K. Aramaki, Effect of molecular weight of triglycerides on the formation and rheological behavior of cubic and hexagonal phase based gel emulsions, J. Colloid Interface Sci. 336 (2009) 329–334. https://doi.org/10.1016/j.jcis.2009.03.054.

[13] C. Azémard, M.C. Fauré, S. Stankic, S. Chenot, H. Ibrahim, L. Laporte, P. Fontaine, M. Goldmann, L. de Viguerie, Influence of Unsaturations on the Organization and Air Reactivity of Triglyceride Monolayers, Langmuir. 38 (2022) 711–718. https://doi.org/10.1021/acs.langmuir.1c02613.

[14] C.C. Akoh, Food Lipids: Chemistry, Nutrition, and Biotechnology, Fourth Edition, CRC Press, 2017.

[15] N.C. Acevedo, A.G. Marangoni, Nanostructured Fat Crystal Systems, Annu. Rev. Food Sci. Technol. 6 (2015) 71–96. https://doi.org/10.1146/annurev-food-030713-092400.

[16] K. Sato, Crystallization behaviour of fats and lipids — a review, Chem. Eng. Sci. 56 (2001) 2255–2265. https://doi.org/10.1016/S0009-2509(00)00458-9.

[17] K. Sato, S. Ueno, Crystallization, transformation and microstructures of polymorphic fats in colloidal dispersion states, Curr. Opin. Colloid Interface Sci. 16 (2011) 384–390. https://doi.org/10.1016/j.cocis.2011.06.004.

[18] A.G. Marangoni, N. Acevedo, F. Maleky, E. Co, F. Peyronel, G. Mazzanti, B. Quinn, D. Pink, Structure and functionality of edible fats, Soft Matter. 8 (2012) 1275–1300. https://doi.org/10.1039/C1SM06234D.

[19] B.S. Ghotra, S.D. Dyal, S.S. Narine, Lipid shortenings: a review, Food Res. Int. 35 (2002) 1015–1048. https://doi.org/10.1016/S0963-9969(02)00163-1.

[20] O.O. Mykhaylyk, I.W. Hamley, The Packing of Triacylglycerols from SAXS Measurements: Application to the Structure of 1,3-Distearoyl-2-oleoyl-sn-glycerol Crystal Phases, J. Phys. Chem. B. 108 (2004) 8069–8083. https://doi.org/10.1021/jp0379704.

[21] C. Lopez, F. Lavigne, P. Lesieur, C. Bourgaux, M. Ollivon, Thermal and Structural Behavior of Milk Fat. 1. Unstable Species of Anhydrous Milk Fat, J. Dairy Sci. 84 (2001) 756–766. https://doi.org/10.3168/jds.S0022-0302(01)74531-6.
[22] P.R. Ramel, E.D. Co, N.C. Acevedo, A.G. Marangoni, Structure and functionality of nanostructured triacylglycerol crystal networks, Prog. Lipid Res. 64 (2016) 231–242. https://doi.org/10.1016/j.plipres.2016.09.004.
[23] B.A. Macias-Rodriguez, A.A. Marangoni, Linear and nonlinear rheological behavior of fat crystal networks, Crit. Rev. Food Sci. Nutr. 58 (2018) 2398–2415. https://doi.org/10.1080/10408398.2017.1325835.
[24] T. Nikolaeva, R. den Adel, E. Velichko, W.G. Bouwman, D. Hermida-Merino, H.V. As, A. Voda, J. van Duynhoven, Networks of micronized fat crystals grown under static conditions, Food Funct. 9 (2018) 2102–2111. https://doi.org/10.1039/C8FO00148K.
[25] L. De Viguerie, G. Ducouret, M. Cotte, F. Lequeux, P. Walter, New insights on the glaze technique through reconstruction of old glaze medium formulations, Colloids Surf. Physicochem. Eng. Asp. 331 (2008) 119–125.
[26] J. Salvant Plisson, L. de Viguerie, L. Tahroucht, M. Menu, G. Ducouret, Rheology of white paints: How Van Gogh achieved his famous impasto, Colloids Surf. Physicochem. Eng. Asp. 458 (2014) 134–141. https://doi.org/10.1016/j.colsurfa.2014.02.055.
[27] I. Bonaduce, L.A. Carlyle, M.P. Colombini, C. Duce, C. Ferrari, E. Ribechini, P. Selleri, M.R. Tiné, A multi-analytical approach to studying binding media in oil paintings, J. Therm. Anal. Calorim. 107 (2012) 1055–1066. https://doi.org/10.1007/s10973-011-1586-6.
[28] T.F. Tadros, Colloids in Paints, John Wiley & Sons, 2011.
[29] Y. Li, A.S. Fabiano-Tixier, K. Ruiz, A. Rossignol Castera, P. Bauduin, O. Diat, F. Chemat, Comprehension of direct extraction of hydrophilic antioxidants using vegetable oils by polar paradox theory and small angle X-ray scattering analysis, Food Chem. 173 (2015) 873–880. https://doi.org/10.1016/j.foodchem.2014.10.061.
[30] C.V. Kulkarni, W. Wachter, G. Iglesias-Salto, S. Engelskirchen, S. Ahualli, Monoolein: a magic lipid?, Phys. Chem. Chem. Phys. 13 (2011) 3004–3021. https://doi.org/10.1039/C0CP01539C.
[31] J.J. Hermans, K. Keune, A. Van Loon, M.J.N. Stols-Witlox, R.W. Corkery, P.D. Iedema, The synthesis of new types of lead and zinc soaps: A source of information for the study of oil paint degradation, in: Build. Strong Cult. Conserv., J. Bridgland, Melbourne, 2014: pp. 1603–1612.
[32] F.J. Martínez-Casado, M. Ramos-Riesco, J.A. Rodríguez-Cheda, M.I. Redondo-Yélamos, L. Garrido, A. Fernández-Martínez, J. García-Barriocanal, I. da Silva, M. Durán-Olivencia, A. Poulain, Lead soaps: crystal structures, polymorphism, and solid and liquid mesophases, Phys. Chem. Chem. Phys. 19 (2017) 17009–17018. https://doi.org/10.1039/C7CP02351K.
[33] S. Koschoreck, S. Fujii, W. Richtering, Shear Induced Structures in Lamellar Systems: From Layers to Onions to Onions and Layers, Prog. Theor. Phys. Suppl. 175 (2008) 154–165. https://doi.org/10.1143/PTPS.175.154.
[34] J.A. Pople, I.W. Hamley, J.P.A. Fairclough, A.J. Ryan, G. Hill, C. Price, A shear induced transition of lamellar alignment in a concentrated diblock copolymer solution, Polymer. 40 (1999) 5709–5714. https://doi.org/10.1016/S0032-3861(98)00805-2.
[35] T. Kato, Shear-Induced Lamellar/Onion Transition in Surfactant Systems, in: A. Iglič, M. Rappolt, A.J. García-Sáez (Eds.), Adv. Biomembr. Lipid Self-Assem., Academic Press, 2018: pp. 187–222. https://doi.org/10.1016/bs.abl.2017.12.006.
[36] M. Lísal, J.K. Brennan, Alignment of Lamellar Diblock Copolymer Phases under Shear: Insight from Dissipative Particle Dynamics Simulations, Langmuir. 23 (2007) 4809–4818. https://doi.org/10.1021/la063095c.
[37] P. Poulin, R. Jalili, W. Neri, F. Nallet, T. Divoux, A. Colin, S.H. Aboutalebi, G. Wallace, C. Zakri, Superflexibility of graphene oxide, Proc. Natl. Acad. Sci. 113 (2016) 11088–11093. https://doi.org/10.1073/pnas.1605121113.

[38] S.R. Ren, I.W. Hamley, G.J.A. Sevink, A.V. Zvelindovsky, J.G.E.M. Fraaije, Mesoscopic Simulations of Lamellar Orientation in Block Copolymers, Macromol. Theory Simul. 11 (2002) 123–127. https://doi.org/10.1002/1521-3919(20020201)11:23.3.CO;2-D.
[39] L. Schneider, M. Müller, Rheology of symmetric diblock copolymers, Comput. Mater. Sci. 169 (2019) 109107. https://doi.org/10.1016/j.commatsci.2019.109107.
[40] A. Guinier, La diffraction des rayons X aux très petits angles : application à l'étude de phénomènes ultramicroscopiques, Ann. Phys. 11 (1939) 161–237. https://doi.org/10.1051/anphys/193911120161.
[41] C.M. Jeffries, J. Ilavsky, A. Martel, S. Hinrichs, A. Meyer, J.S. Pedersen, A.V. Sokolova, D.I. Svergun, Small-angle X-ray and neutron scattering, Nat. Rev. Methods Primer. 1 (2021) 1–39. https://doi.org/10.1038/s43586-021-00064-9.
[42] G. Fritz, N.J. Wagner, E.W. Kaler, Formation of Multilamellar Vesicles by Oscillatory Shear, Langmuir. 19 (2003) 8709–8714. https://doi.org/10.1021/la0349370.
[43] O. Diat, D. Roux, Preparation of monodisperse multilayer vesicles of controlled size and high encapsulation ratio., J. Phys. II. 3 (1993) 9–14. https://doi.org/10.1051/jp2:1993106.
[44] M.G. Berni, C.J. Lawrence, D. Machin, A review of the rheology of the lamellar phase in surfactant systems, Adv. Colloid Interface Sci. 98 (2002) 217–243. https://doi.org/10.1016/S0001-8686(01)00094-X.
[45] M. Ito, Y. Kosaka, Y. Kawabata, T. Kato, Transition processes from the lamellar to the onion state with increasing temperature under shear flow in a nonionic surfactant/water system studied by Rheo-SAXS, Langmuir ACS J. Surf. Colloids. 27 (2011) 7400–7409. https://doi.org/10.1021/la104826s.
[46] A. Guinier, G. Fournet, Small-angle Scattering of X-rays, Wiley, 1955.
[47] J.S. Pedersen, Analysis of small-angle scattering data from colloids and polymer solutions: modeling and least-squares fitting, Adv. Colloid Interface Sci. 70 (1997) 171–210. https://doi.org/10.1016/S0001-8686(97)00312-6.
[48] H.A. Ellis, N.A.S. White, R.A. Taylor, P.T. Maragh, Infrared, X-ray and microscopic studies on the room temperature structure of anhydrous lead (II) n-alkanoates, J. Mol. Struct. 738 (2005) 205–210. https://doi.org/10.1016/j.molstruc.2004.12.006.
[49] F.J. Martínez-Casado, J.A. Rodríguez-Cheda, M. Ramos-Riesco, M.I. Redondo-Yélamos, F. Cucinotta, A. Fernández-Martínez, in: F. Casadio, K. Keune, P. Noble, A. Van Loon, E. Hendriks, S.A. Centeno, G. Osmond (Eds.), Physicochem. Pure LeadII Soaps Cryst. Struct. Solid Liq. Mesophases Glass Phases – Crystallogr. Calorimetric Pair Distrib. Funct. Anal., Springer International Publishing, Cham, 2019. https://doi.org/10.1007/978-3-319-90617-1_13.

Captions

Supporting Information

Figure 1: Linseed oil + 50 mol% PbO - evolution of viscosity as a function of shear rate, ramp up and ramp down. Each shear rate value was applied for 60 minutes.

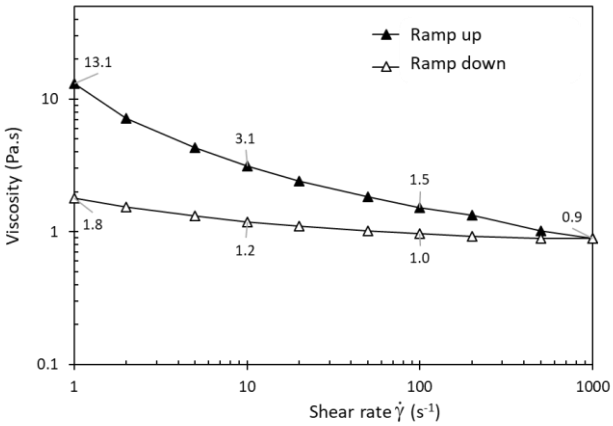

Figure 2: (a) Evolution of G' and G'' after oscillatory shear from 0.1 to 1000 % strain on linseed oil + 50 % PbO for 16h after the end of shear. Solid straight lines represent the initial values of G' and G'' at 0.5% strain, before shearing. (b) Detail on the evolution of G' and G'' (γ = 0.5%, f = 1 Hz) from 0 to 240 minutes after the end of shearing.

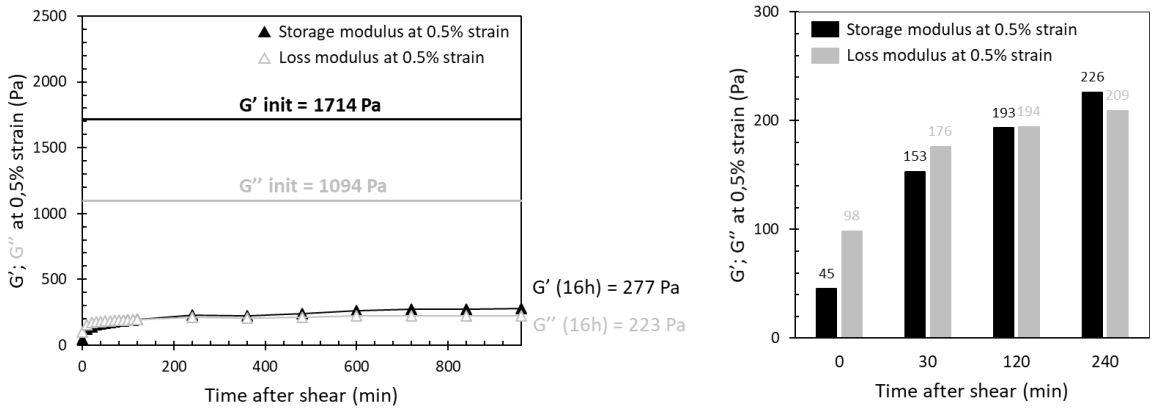

Figure 3: Evolution of azimuthal profiles under continuous shear for linseed oil + 17 mol% PbO. The "r" refers to shear rate values applied on ramp down.

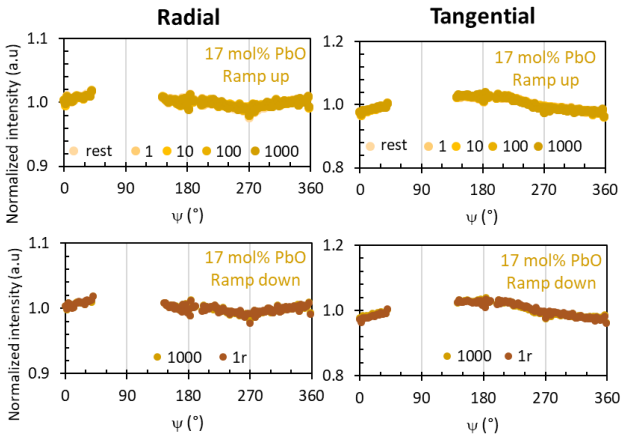

Figure 4: (a) Linseed oil + 50 mol% PbO - azimuthal integration evolution in radial configuration, from 20 to 1000% strain at f=1Hz. (b) Radius of gyration measured by applying a Guinier fit in the 0.01 to 0.10 Å^{-1} *q-range*, from 0.05 to 1000% strain. Above 20% strain, the growth of the objects is limited.

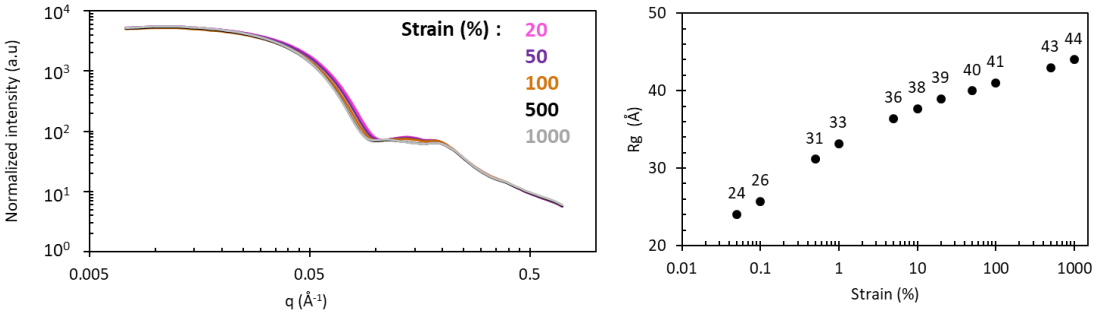

(a) (b)

Figure 5: Linseed oil + 50 mol% PbO - azimuthal profile evolution in radial and tangential configurations from 0 to 30 minutes after the end of the oscillatory shear. Vertical orientation was still detected 30minutes after the end of shearing in both configurations.

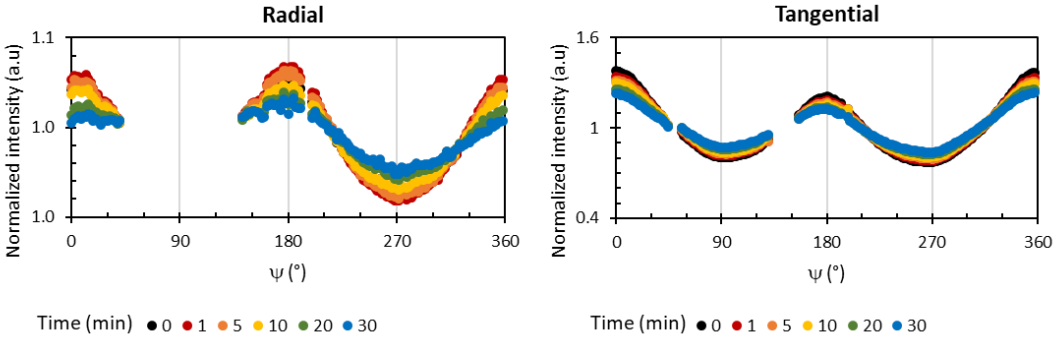

Figure 6: Linseed oil + 50 mol% PbO – (a) azimuthal integration evolution in radial configuration from 0 to 30 minutes after the end of the oscillatory shear. (b) Radius of gyration measured by applying a Guinier fit in the 0.01 to 0.10 Å^{-1} *q-range*. No more growth of cylindrical objects was observed.

(a)

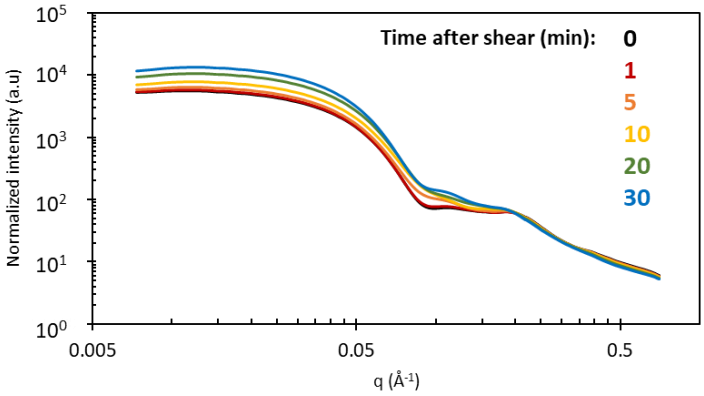

(b)

Time after shear (min)	0	1	5	10	20	30
Rg (Å)	44	44	44	43	44	45